SCIENTIFIC OASIS

Decision Making: Applications in Management and Engineering

Journal homepage: www.dmame-journal.org
ISSN: 2560-6018, eISSN: 2620-0104

A Decision-Support Framework for Composite Curved Beam Design under Moving Loads: Dynamic Modelling and Multi-Criteria Evaluation

Nihayat Hussein Ameen[1*]

1 BA, College of agriculture, Kirkuk University, Iraq. ORCID: https://orcid.org/0000-0001-5997-5759

ARTICLE INFO

Article history:
Received 1 January 2025
Received in revised form 5 June 2025
Accepted 10 July2025
Available online 10 August 2025

Keywords:
Curved Beam, Dynamic Response, Moving Mass, Composite Beam, Navier Solution, Design Choices, MCDM

ABSTRACT

Behavior of curved beams subjected to moving loads has specific application in the structural design of bridges, railways, as well as machining frames. With the growth in applications of the composite material in structural members, in the form of beams, plates, as well as in columns, the stringent analysis of their transient loading behavior has been made inevitable. This paper investigates the dynamics of a moderately deep, orthotropic curved composite beam subjected to moving mass loads. Analysis is based on the first-order shear deformation theory in combination with Hamilton's principle, for the identification of the governing partial differential equations in the spatial as well as time domains. These equations are then reduced to ordinary differential equations in the spatial domain using Navier's method, while the temporal aspect is resolved using Newmark's numerical integration scheme. The accuracy of the model's natural frequency predictions is validated through comparison with both straight and curved composite beam configurations, as well as with cases involving moving mass loads, demonstrating strong agreement with previously published results. In practical engineering scenarios, particularly in high-speed railway systems and aerospace structures, selecting the optimal configuration of curved composite beams necessitates careful consideration of factors such as stiffness, weight, manufacturability, and resilience to dynamic loading. The study reveals that increasing the mass and length of the beam leads to a notable amplification in its dynamic response. Additionally, the stacking sequence and orientation of the composite layers play a decisive role in influencing vibrational behaviour. Nonetheless, the configuration of the layers profoundly affects the dynamic responding related to the beam curved counting on a moving mass, with the amplitude of structural oscillations being maximized for layers and minimized for layers. To support optimal design strategies, a Multi-Criteria Decision-Making (MCDM) framework is introduced, enabling a structured evaluation of trade-offs among structural stiffness, mass, cost, and vibration performance. The findings underscore the necessity of such a decision-making tool in selecting optimal beam configurations under realistic dynamic loading conditions, considering variables such as load velocity, curvature, and anisotropic material behaviour. This research offers practical guidance for engineers in choosing suitable laminate architectures and materials to reduce vibration and enhance durability in transportation and civil engineering infrastructure. The study contributes to informed decision-making in high-speed rail and aerospace applications, where control of dynamic performance is of critical importance.

* *Corresponding author.*
E-mail address: 320220944270@lzu.edu.cn

https://doi.org/10.31181/dmame8220251479

1. Introduction

Composite curved structures, initially developed for aerospace rings, have progressively expanded their applications into civil engineering, particularly in arch-based systems. Their unique capability to efficiently support dynamic moving loads has rendered them increasingly significant in contemporary structural engineering practice [21]. These structures are commonly utilised across various sectors, including transportation, industrial automation, and robotics, where interaction with moving masses—such as vehicles, robotic payloads, or heavy machinery—is prevalent [38]. In contrast, straight beams exhibit comparatively simpler dynamic responses due to limited coupling among axial, flexural, and torsional vibrations, resulting in more predictable behaviour under dynamic excitation [11]. The intrinsic complexity of curved structural elements has prompted the development of extensive analytical models aimed at accurately characterising their behaviour under diverse dynamic conditions [3]. Modern infrastructure and transportation systems demand highly accurate and reliable structural performance, particularly in the face of increasing operational velocities, heavier loads, and higher safety and efficiency requirements [1]. Consequently, there is an urgent requirement for advanced investigation into the dynamic responses of composite curved structures subjected to moving mass scenarios [12].

Early foundational work, such as that by Smith on elongated strings interacting with moving masses, contributed significantly to understanding mass-motion dynamics [10]. However, limited focus has been directed towards more sophisticated systems, particularly curved composite structures under non-stationary dynamic loading. This creates a knowledge gap requiring renewed investigation into the distinctive behaviours of such composites and their implications for structural design and material engineering [20]. Recent progress in dynamic modelling of curved composites using high-fidelity techniques presents substantial potential. For example, the elasto-dynamic response of curved sandwich beams under moving mass loads was analysed using Finite Element Method (FEM), highlighting notable interactions between geometry and inertial effects [10]. Advanced theories, such as higher-order shear deformation, have also been applied to examine the dynamic stability of stiffened curved plates, demonstrating dependence on velocity and stiffness gradients [26]. These outcomes have shown consistency with simulations based on variable curvature and multi-parameter beam formulations [18].

Functionally graded materials (FGMs) and porous composites have become crucial in enhancing vibration control performance, especially under moving mass effects, due to their tuneable stiffness, mass distribution, and damping characteristics [25]. FGMs offer precise design flexibility, enabling engineers to optimise vibrational responses and improve structural reliability and longevity [15]. Notably, the dynamic response of elliptically curved steel beams under varying-speed moving mass loads was successfully controlled through FGM configurations [30]. Despite these benefits, the complex vibration behaviours encountered in real-world engineering applications continue to pose both challenges and opportunities for material innovation [18].

Additionally, finite element approximations have shown effectiveness in modelling acceleration-induced deflections in beams under time-dependent loads [4]. These methods have also proven capable of capturing non-uniform spatial curvature variations, encouraging the integration of advanced composite materials for enhanced vibration suppression [31]. Collectively, these research outcomes emphasise the pivotal role that FGMs and porous composites play in modern structural engineering while offering essential theoretical insights for improving the accuracy of dynamic response predictions under challenging operational conditions [34]. Recent observations also indicate a marked increase in the frequency of high-speed overloaded lorries, intensifying concerns over dynamic mass interactions with structural materials in roadways and bridges [22]. The materials used in such infrastructures must balance strength and lightness, which is why

composites—owing to their high strength-to-weight ratio—are proving to be highly efficient in bridges, buildings, and industrial structures [2; 5]. Finite element investigations of asymmetric multilayer composite beams subjected to fluctuating loads have been carried out to understand their performance [14]. The dynamic contribution of the moving mass can be disregarded if its magnitude is negligible in comparison to the structural mass, simplifying the analysis [33]. However, the presence of moving masses introduces inertia effects that complicate the governing equations, often preventing the derivation of exact solutions [36]. To address this, a modified FEM has been proposed for evaluating the longitudinal vibrations of Timoshenko beams composed of FGMs, under moving masses with variable velocity, considering dual-parameter modelling [9]. In another study, the free and forced vibration behaviour of porous beams, featuring spatially non-uniform porosity distributions and nonlinear variations in elastic moduli and density across the thickness, was investigated [7]. Further, the transient and free vibration responses of simply supported beams under dynamic concentrated harmonic loading have been studied, offering key insights into structural behaviour [29].

The quasi-three-dimensional shear deformation theory was employed to analyse the dynamic behaviour of sandwich beams with porous cores and carbon nanotube-reinforced polymer face sheets under moving mass loading [6]. Using Euler-Bernoulli theory, the vibration and instability of curved beams with varied boundary conditions under moving mass loading were also evaluated, including the instability mechanisms arising in vehicles on curved paths [19]. A broader set of governing equations for curved beam motion—encompassing vertical, torsional, radial, and axial components—was derived using the Lagrangian method by accounting for bending stiffness and inertia forces. It was shown that in angular porcelain layers, the dynamic response of the beam increases with the fibre orientation angle [17]. In practical engineering settings, particularly in transportation infrastructure, the selection of optimal curved composite beam configurations requires careful consideration of trade-offs among weight, stiffness, manufacturing constraints, and stability under dynamic loading. Civil engineers must assess various laminate stacking sequences, geometric curvatures, and material properties to ensure a balance between performance, durability, and cost-effectiveness. Previous studies have highlighted the importance of simulation-based structural optimisation in high-speed railway and aerospace systems, where transient loading and vibration control are critical design parameters [27; 35].

These challenges underscore the necessity of a robust decision-making framework to support the rational selection of composite structures in dynamic operating environments [23]. Composite curved beams are increasingly implemented in bridges and high-speed transport systems because of their favourable mechanical properties and design adaptability. Nonetheless, the selection of an ideal configuration remains complex due to the interplay among anisotropic material behaviour, geometric parameters, and dynamic forces [37]. Accordingly, engineering decisions must be underpinned by validated numerical models capable of predicting dynamic responses across design variables, including curvature radius, load velocity, laminate orientation, and mass ratio [16]. This research addresses a notable gap in the current literature concerning the dynamic behaviour of composite curved beams under non-uniform mass loading. The present study applies first-order shear deformation theory to derive the governing equations, which are then solved using the Newmark method. Key influencing factors such as beam speed, geometric dimensions, curvature, and laminate stacking sequence are evaluated. Hamilton's principle is employed as the foundational framework for deriving the system's equations of motion. The research is positioned not only as a modelling task but also as a contribution to structural design decision-making. By simulating the performance of various curved composite beam configurations under dynamic mass loading, the study offers insights to inform trade-offs in structural optimisation. It ultimately bridges the divide

between analytical simulation and practical engineering design.

2. Structure Modelling

Figure 1 presents a schematic representation of a layered composite beam featuring a constant breadth b and thickness h. The curvature of the beam is assumed to remain constant over its entire arc. The radius of curving and the arc angle of the beam are effectively pointed out by R and θ_0, correspondingly. The beam's mid surface is marked with the three coordinates x, y, and z, which represent the longitudinal, transverse, and thickness sides, respectively. The displacements u and w are associated with the x and z sides, respectively, while ϕ represents the spinning of the beam's cross-section around the y axis. As illustrated in Figure 1, the beam is subjected to simple support boundary conditions and is analysed under the influence of a moving mass m travelling at a constant velocity v. The composite beam comprises multiple orthotropic layers, all of which are assumed to be perfectly bonded, ensuring integrated mechanical interaction across the laminate. The moving mass is considered to remain in uninterrupted contact with the beam throughout its motion, with no possibility of detachment during the loading process. Additionally, the structural model omits damping effects, under the assumption that such influences are sufficiently small to be neglected within the scope of this analysis.

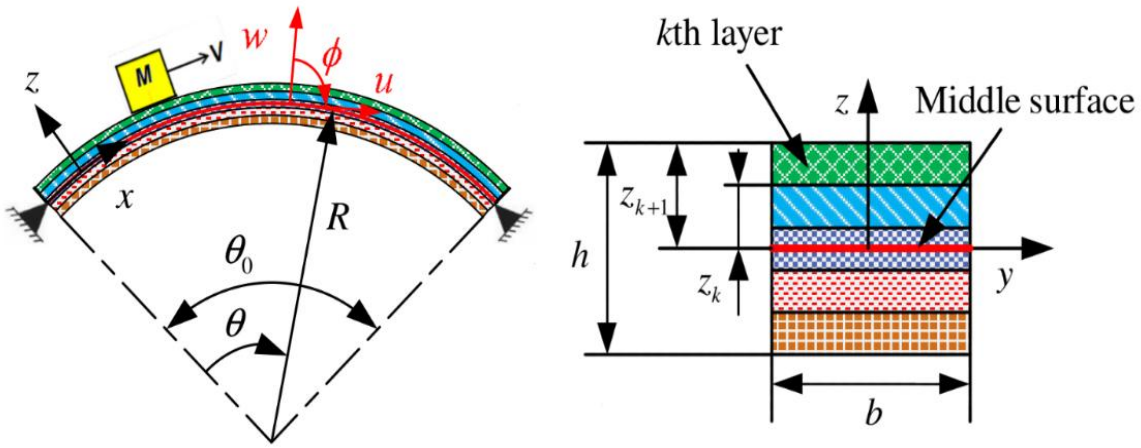

Fig.1: Diagram of the Composite Curving Beam and Coordinates Display System.

2.1 Composite Curved Beam Displacement Field

The governing differential equations for the composite curved beam have been formulated based on first-order shear deformation theory. The total displacements in the longitudinal and transverse directions for an arbitrary point within the composite curved beam are assumed to follow the expressions outlined in [28].

$$\begin{aligned} u(x,z,t) &= u_0(x,t) + z\phi(x,t) \\ w(x,z,t) &= w_0(x,t) \end{aligned} \tag{1}$$

The mid surface displacement for x and y, respectively, is represented by u_0 and w_0. As presented in [2], the vertical and shear strain components at an arbitrary point along the beam are defined as follows:

$$\varepsilon_x = \frac{1}{1+\frac{z}{R}}\left(\varepsilon_x^0 + z\varepsilon_x^1\right)$$
$$\gamma_{xz} = \frac{1}{1+\frac{z}{R}}\gamma_{xz}^0 \tag{2}$$

where ε_x^1 denotes curvature changes, and ε_x^0, γ_{xz}^0 are the vertical and shear strain in the mid surface, respectively, as follows:

$$\varepsilon_x^0 = \frac{\partial u_0}{\partial x} + \frac{w_0}{R}$$
$$\varepsilon_x^1 = \frac{\partial \phi}{\partial x} \tag{3}$$
$$\gamma_{xz}^0 = \frac{\partial w_0}{\partial x} - \frac{u_0}{R} + \phi$$

Assuming that $x = R\theta$ and $dx = Rd\theta$:

$$\varepsilon_\theta^0 = \frac{\partial u_0}{R\partial \theta} + \frac{w_0}{R}$$
$$\varepsilon_\theta^1 = \frac{\partial \phi}{R\partial \theta} \tag{4}$$
$$\gamma_{\theta z}^0 = \frac{\partial w_0}{R\partial \theta} - \frac{u_0}{R} + \phi$$

In accordance with Hooke's law, the stress–strain relationship within layer k of the curved laminated beam is expressed as follows:

$$\begin{Bmatrix} \sigma_\theta \\ \tau_{\theta z} \end{Bmatrix}_k = \begin{bmatrix} E_x^k & 0 \\ 0 & \bar{Q}_{55}^k \end{bmatrix} \begin{Bmatrix} \varepsilon_\theta \\ \gamma_{\theta z} \end{Bmatrix}_k \tag{5}$$

Where σ_θ and $\tau_{\theta z}$ represent vertical and shear stresses, respectively. E_x^k is the equivalent elasticity modulus of each stratum, and $\bar{Q}_{55}^k$ is the transformed elastic stiffness coefficient, as defined in [18]:

$$\frac{1}{E_x^k} = \frac{\cos^4\left(\alpha^k\right)}{E_{11}} + \left(\frac{1}{G_{12}} - \frac{2\upsilon_{12}}{E_{11}}\right)\cos^2\left(\alpha^k\right)\sin^2\left(\alpha^k\right) + \frac{\sin^4\left(\alpha^k\right)}{E_{22}}$$
$$\bar{Q}_{55}^k = G_{13}\cos^2\left(\alpha^k\right) + G_{23}\sin^2\left(\alpha^k\right) \tag{6}$$

Where α^k stands for the angle among the x-axis and the fibres of the kth stratum. The elastic modulus E_{22} is the moduli of elasticity of the composites in perpendicularly to the fibres, while E_{11} is the modulus of elasticity in the side of the fibres. Poisson's ratio is denoted by υ_{12}, while shear modulus is represented by G_{13}, G_{12}, and G_{23}.

2.2 Relations of Energy

The curved beam's strain energy is described as follows:

$$U=\frac{1}{2}\int_0^{\theta_0}\int_{-\frac{h}{2}}^{\frac{h}{2}} b\left[\sigma_\theta\varepsilon_\theta+\sigma_{\theta z}\gamma_{\theta z}^0\right](1+\frac{z}{R})R\mathrm{d}z\mathrm{d}\theta=$$
$$\frac{1}{2}\int_0^{\theta_0}\left[N_\theta\varepsilon_\theta^0+\bar{M}_\theta\varepsilon_\theta^1+Q_\theta\gamma_{\theta z}^0\right]R\mathrm{d}\theta \tag{7}$$

The corresponding expressions for the resultant forces and moments derived from the aforementioned stress–strain relationship are obtained as follows:

$$N_\theta=b\sum_{k=1}^{n}\int_{z_k}^{z_{k+1}}\sigma_\theta dz,\bar{M}_\theta=b\sum_{k=1}^{n}\int_{z_k}^{z_{k+1}}\sigma_\theta z dz,Q_\theta=b\sum_{k=1}^{n}\int_{z_k}^{z_{k+1}}\tau_{\theta z}dz \tag{8}$$

Where Q_θ and $\bar{M}_\theta$ stand for shear force and curving moment, respectively, and N_θ represents axial force. In Figure 1, the coordinates of the lowest and highest point of the kth layer are represented by z_k and z_{k+1}, and n is (level No).

The relationship between the internal forces and moments with respect to variations in curvature, shear strain, and normal strain is obtained by substituting equation (5) into equation (8):

$$\begin{bmatrix}N_\theta\\ \bar{M}_\theta\\ Q_\theta\end{bmatrix}=\begin{bmatrix}A_{11} & B_{11} & 0\\ B_{11} & D_{11} & 0\\ 0 & 0 & A_{55}\end{bmatrix}\begin{bmatrix}\varepsilon_\theta^0\\ \varepsilon_\theta^1\\ \gamma_{\theta z}^0\end{bmatrix} \tag{9}$$

Where the stiffness coefficients A_{11}, B_{11}, D_{11}, and A_{55} are denoted as:

$$A_{11}=Rb\sum_{k=1}^{n}E_x^k\ln\left(\frac{R+z_{k+1}}{R+z_k}\right)$$
$$B_{11}=Rb\sum_{k=1}^{n}E_x^k\left[\left(z_{k+1}-z_k\right)-R\ln\left(\frac{R+z_{k+1}}{R+z_k}\right)\right]$$
$$D_{11}=Rb\sum_{k=1}^{n}E_x^k\left[\begin{array}{l}\frac{1}{2}\left((R+z_{k+1})^2-(R+z_k)^2\right)-2R\left(z_{k+1}-z_k\right)\\ +R^2\ln\left(\frac{R+z_{k+1}}{R+z_k}\right)\end{array}\right] \tag{10}$$
$$A_{55}=\frac{5}{4}b\sum_{k=1}^{n}\bar{Q}_{55}^k\left[\left(z_{k+1}-z_k\right)-\frac{4}{3h^2}\left(z_{k+1}^3-z_k^3\right)\right]$$

Accordingly, the strain energy of the curved composite beam is represented as follows:

$$U=\frac{1}{2}\int_0^{\theta_0}\left[\begin{array}{l}A_{11}\left(\frac{\partial u_0}{R\partial(\theta)}+\frac{w_0}{R}\right)^2+2B_{11}\frac{\partial\phi}{R\partial(\theta)}\left(\frac{\partial u_0}{R\partial(\theta)}+\frac{w_0}{R}\right)+D_{11}\left(\frac{\partial\phi}{R\partial(\theta)}\right)^2\\ +A_{55}\left(\frac{\partial w_0}{R\partial(\theta)}-\frac{u_0}{R}+\phi\right)^2\end{array}\right]R\mathrm{d}\theta \tag{11}$$

The kinetic energy of the curved beam is defined as follows:

$$T=\frac{b}{2}\int_0^{\theta_0}\int_{-\frac{h}{2}}^{\frac{h}{2}}\rho\left[\left(\frac{\partial u_0}{\partial t}+z\frac{\partial\phi}{\partial t}\right)^2+\left(\frac{\partial w_0}{\partial t}\right)^2\right](1+\frac{z}{R})R\mathrm{d}\theta\ \mathrm{d}z+\frac{1}{2}M\left|V_{Tot}\right|^2$$
$$=\frac{b}{2}\int_0^{\theta_0}\left[\begin{array}{l}\left(I_0+\frac{I_1}{R}\right)\left(\frac{\partial u_0}{\partial t}\right)^2+2\left(I_1+\frac{I_2}{R}\right)\left(\frac{\partial u_0}{\partial t}\frac{\partial\phi}{\partial t}\right)\\+\left(I_2+\frac{I_3}{R}\right)\left(\frac{\partial\phi}{\partial t}\right)^2+\left(I_0+\frac{I_1}{R}\right)\left(\frac{\partial w_0}{\partial t}\right)^2\end{array}\right]R\mathrm{d}\theta+\frac{1}{2}M\left|V_{Tot}\right|^2 \quad (12)$$

Where $|V_{Tot}|$ is the total absolute speed, which encompasses both linear and rotational factors. Additionally:

$$\begin{aligned}&\bar{I}_1=I_0+\frac{I_1}{R}\\&\bar{I}_2=I_1+\frac{I_2}{R}\quad\rightarrow\left[I_0,I_1,I_2,I_3\right]=b\sum_{k=1}^{n}\int_{z_k}^{z_{k+1}}\rho^k\left[1,z,z^2,z^3\right]\mathrm{d}z\\&\bar{I}_3=I_2+\frac{I_3}{R}\end{aligned} \quad (13)$$

2.3 Hamilton's Principle

This principle is effectively applied to derive the governing equations for the composite curved beam, as outlined in [35]:

$$\int_0^t(\delta U+\delta W-\delta T)dt=0 \quad (14)$$

T, U, and W show the locomotive energy, straining latent vigour, and work of outer forces, correspondingly.

The following equation describes the variation in the dynamic energy of the composite curved beam as the moving mass M travels along the beam at a constant horizontal velocity V.

$$\begin{aligned}&\int_{t_1}^{t_2}\delta T\mathrm{d}t=-\int_{t_1}^{t_2}\int_0^{\theta_0}\left[\bar{I}_1\ddot{u}_0\delta u_0+\bar{I}_2\ddot{u}_0\delta\phi+\bar{I}_2\ddot{\phi}\delta u_0+\bar{I}_3\ddot{\phi}\delta\phi+\bar{I}_1\ddot{w}_0\delta w_0\right]R\mathrm{d}\theta\mathrm{d}t\\&+\left[M\frac{V^2}{R}-\int_{t_1}^{t_2}\int_0^{\theta_0}M\left(V^2w_0''+2V\dot{w}_0'+\ddot{w}_0\right)\right]\delta w_0\delta_D\left(R\theta-Vt\right)R\mathrm{d}\theta\mathrm{d}t\end{aligned} \quad (15)$$

The variations in the strain energy of the curved beam are given as follows:

$$\begin{aligned}&\int_{t_1}^{t_2}\delta U dt=\int_{t_1}^{t_2}\int_0^{\theta_0}\left(A_{11}\left(\frac{\partial u_0}{R\partial\theta}+\frac{w_0}{R}\right)+B_{11}\frac{\partial\phi}{R\partial\theta}\right)\frac{\delta\partial u_0}{\partial\theta}+\left(A_{11}\left(\frac{\partial u_0}{R\partial\theta}+\frac{w_0}{R}\right)+B_{11}\frac{\partial\phi}{R\partial\theta}\right)\delta w_0\\&+\left(B_{11}\left(\frac{\partial u_0}{R\partial\theta}+\frac{w_0}{R}\right)+D_{11}\frac{\partial\phi}{R\partial\theta}\right)\frac{\delta\partial\phi}{\partial\theta}+\left(A_{55}\left(\frac{\partial w_0}{R\partial\theta}-\frac{u_0}{R}+\phi\right)\right)\frac{\delta\partial w_0}{\partial\theta}R\delta\phi\\&-\left(A_{55}\left(\frac{\partial w_0}{R\partial\theta}-\frac{u_0}{R}+\phi\right)\right)\delta u_0+\left(A_{55}\left(\frac{\partial w_0}{R\partial\theta}-\frac{u_0}{R}+\phi\right)\right)\mathrm{d}\theta\mathrm{d}t\end{aligned} \quad (16)$$

The variation in energy resulting from the external action of the moving mass M on the specified composite curved beam is expressed as follows:

$$\int_{t_1}^{t_2}\delta W_M \mathrm{d}t = -\int_{t_1}^{t_2}\int_0^{\theta_0} Mg\cos\left(\frac{\theta_0}{2}-\theta\right)\delta_D\left(R\theta-Vt\right)\delta w_0 R\mathrm{d}\theta\mathrm{d}t+$$
$$\int_{t_1}^{t_2}\int_0^{\theta_0} Mg\sin\left(\frac{\theta_0}{2}-\theta\right)\delta_D\left(R\theta-Vt\right)\delta u_0 R\mathrm{d}\theta\mathrm{d}t \tag{17}$$

In the aforementioned connection, δ_D represents Dirac's delta function.

By substituting the relationships obtained from equation (14), carrying out the standard spatial and temporal integrations, and subsequently simplifying, the governing equations for the composite curved beam are effectively formulated in terms of the displacement field components.

δu_0 :

$$R\bar{I}_1\ddot{u}_0 + R\bar{I}_2\ddot{\phi} - \frac{1}{R}A_{11}\frac{\partial^2 u_0}{\partial\theta^2} - \frac{1}{R}A_{11}\frac{\partial w_0}{\partial\theta} - \frac{1}{R}B_{11}\frac{\partial^2\phi}{\partial\theta^2} - \frac{1}{R}A_{55}\frac{\partial w_0}{\partial\theta} + \frac{1}{R}A_{55}u_0 - A_{55}\phi$$
$$-RMg\sin\left(\frac{\theta_0}{2}-\theta\right)\delta_D\left(R\theta-Vt\right)=0 \tag{18}$$

δw_0 :

$$R\bar{I}_1\ddot{w}_0 + R\left(MV^2 w_0'' - M\frac{V^2}{R} + 2MV\dot{w}_0' + M\ddot{w}_0 + Mg\cos\left(\frac{\theta_0}{2}-\theta\right)\right)\delta_D\left(R\theta-Vt\right)$$
$$+\frac{1}{R}A_{11}\frac{\partial u_0}{\partial\theta} + \frac{1}{R}A_{11}w_0 + \frac{1}{R}B_{11}\frac{\partial\phi}{\partial\theta} - \frac{1}{R}A_{55}\frac{\partial^2 w_0}{\partial\theta^2} + \frac{1}{R}A_{55}\frac{\partial u_0}{\partial\theta} - A_{55}\frac{\partial\phi}{\partial\theta}=0 \tag{19}$$

$\delta\phi$:

$$R\bar{I}_2\ddot{u}_0 + R\bar{I}_3\ddot{\phi} - \frac{1}{R}B_{11}\frac{\partial^2 u_0}{\partial\theta^2} - \frac{1}{R}B_{11}\frac{\partial w_0}{\partial\theta} - \frac{1}{R}D_{11}\frac{\partial^2\phi}{\partial\theta^2} + A_{55}\frac{\partial w_0}{\partial\theta} - A_{55}u_0 + RA_{55}\phi = 0 \tag{20}$$

Considering the insignificance of angle $\left(\frac{\theta_0}{2}-\theta\right)$, the term $RMg\sin\left(\frac{\theta_0}{2}-\theta\right)\delta_D\left(R\theta-Vt\right)$ is disregarded. By performing algebraic manipulations and simplifying the previously established expressions, the partial differential equations governing the motion of the system in the axial, flexural, and radial directions are derived as follows:

δu_0 :

$$\bar{I}_1R^2\frac{\partial^2 u_0}{\partial t^2} + \bar{I}_2R^2\frac{\partial^2\phi}{\partial t^2} - A_{11}\left(\frac{\partial^2 u_0}{\partial\theta^2}+\frac{\partial w_0}{\partial\theta}\right) - B_{11}\frac{\partial^2\phi}{\partial\theta^2} - A_{55}\left(\frac{\partial w_0}{\partial\theta}-u_0+R\phi\right)=0 \tag{21}$$

δw_0 :

$$\bar{I}_1R^2\frac{\partial^2 w_0}{\partial t^2} + A_{11}\left(\frac{\partial u_0}{\partial\theta}+w_0\right) + B_{11}\frac{\partial\phi}{\partial\theta} - A_{55}\left(\frac{\partial^2 w_0}{\partial\theta^2} - \frac{\partial u_0}{\partial\theta} + R\frac{\partial\phi}{\partial\theta}\right)$$
$$+R^2\left[MV^2\frac{\partial^2 w_0}{\partial\theta^2} - M\frac{V^2}{R} + M\frac{\partial^2 w_0}{\partial t^2} + 2MV\frac{\partial^2 w_0}{\partial t\partial\theta}\right]\delta_D\left(R\theta-Vt\right)$$
$$=-R^2Mg\cos\left(\frac{\theta_0}{2}-\theta\right)\delta_D\left(R\theta-Vt\right) \tag{22}$$

$\delta\phi$:

$$\bar{I}_2 R^2 \frac{\partial^2 u_0}{\partial t^2} + \bar{I}_3 R^2 \frac{\partial^2 \phi}{\partial t^2} - B_{11}\left(\frac{\partial^2 u_0}{\partial \theta^2} + \frac{\partial w_0}{\partial \theta}\right) - D_{11}\frac{\partial^2 \phi}{\partial \theta^2} + A_{55}\left(\frac{\partial w_0}{\partial \theta} - u_0 + R\phi\right) = 0 \quad (23)$$

2.4 Exact Solution

This study investigates a simply supported curved composite beam, employing Navier's method to discretise the system's differential equations within the spatial domain. To satisfy the boundary conditions, the displacement field components are defined as follows:

$$\begin{aligned} u_0(\theta,t) &= \sum_{i=1}^{N} u_i(t)\cos\left(\frac{i\pi R\theta}{L}\right) \\ w_0(\theta,t) &= \sum_{i=1}^{N} w_i(t)\sin\left(\frac{i\pi R\theta}{L}\right) \\ \phi(\theta,t) &= \sum_{i=1}^{N} \phi_i(t)\cos\left(\frac{i\pi R\theta}{L}\right) \end{aligned} \quad (24)$$

Where N represents (count of considered modes), L denotes the beam length, and i indicates the required mode number. Furthermore, $u_i(t)$, $w_i(t)$, and $\phi_i(t)$ the generalized coordinates of the structure.

The dynamic response of the curved beam is determined by substituting equations (24) into the equations of motion (21) to (23). Consequently, the resulting differential equations are as follows:

$$[\mathbf{M}]\{\ddot{\mathbf{X}}\} + [\mathbf{C}]\{\dot{\mathbf{X}}\} + [\mathbf{K}]\{\mathbf{X}\} = \{\mathbf{F}\} \quad (25)$$

In the aforementioned connection, $[\mathbf{M}]$ is the mass matrix, $[\mathbf{C}]$ the damping matrix, $[\mathbf{K}]$ the stiffness matrix, $\{\ddot{\mathbf{X}}\}$ the acceleration vector, $\{\dot{\mathbf{X}}\}$ the velocity vector, $\{\mathbf{X}\}$ to the displacement vector, and GH is the force vector.

The analytical solution to the aforementioned problem is obtained using the Newmark central difference method in the time domain.

3. Multi-Criteria Decision-Making (MCDM)

In modern structural engineering, particularly within high-speed railway systems and aerospace applications, selecting the most suitable composite curved beam configuration requires a careful trade-off among several often-conflicting performance factors. These include stability under dynamic loading, structural weight, cost-efficiency, and stiffness performance. To navigate this complexity, a MCDM framework was employed subsequent to the dynamic parametric analysis, enabling a comprehensive assessment and informed selection of optimal beam configurations [24].

3.1 Identification of Decision Criteria

Based on prior analytical simulations and engineering relevance, four core performance indicators were selected as decision criteria:

- Natural Frequency (f): Higher natural frequencies are indicative of enhanced dynamic stability and are thus considered a benefit criterion.
- Static Deflection (δ): Reduced deflection under applied loads reflects superior structural rigidity, making this a cost criterion.

• Mass per Unit Length (M_o): A lower mass per unit length is favourable as it minimises inertial effects and simplifies handling and installation, qualifying it as a cost criterion.

• Estimated Cost (C): Approximated through the product of material density and volume, with lower costs being preferable; this is also classified as a cost criterion.

These selected criteria align with practical engineering priorities in the design of composite structures such as bridge decks, railway components, and aircraft fuselages, where dynamic load performance, durability, and cost-efficiency are critical considerations [8; 13].

3.2 Evaluation Using TOPSIS Method

To evaluate and rank alternative beam configurations, the Technique for Order Preference by Similarity to Ideal Solution (TOPSIS) was employed, given its computational efficiency, scalability, and capability to incorporate both benefit-oriented and cost-oriented criteria [21].

Step 1: Constructing the Decision Matrix

Let $X = [X - ij]$ represent the decision matrix, where each row i is a beam configuration, and each column j is a criterion.

Step 2: Normalizing the Matrix

Each parameter value was subjected to vector normalisation using the following expression:

$$\mathbf{rij} = \frac{\mathbf{x_{ij}}}{\sqrt{\sum_{\boldsymbol{i=j}}^{\boldsymbol{m}} \boldsymbol{x2_{ij}}}} \quad (\mathbf{26})$$

Step 3: Weight Assignment

The normalised values were subsequently weighted to represent the relative significance of each criterion:

$$\mathbf{v\_ij} = \mathbf{w\_j} \cdot \mathbf{r\_ij} \quad (\mathbf{27})$$

Step 4: Determining Ideal and Negative-Ideal Solutions

$$\mathbf{A+} = \{\mathbf{max\ v\_ij} \mid \mathbf{j} \in \mathbf{J\_benefit\ min\ v\_ij} \mid \mathbf{j} \in \mathbf{J\_cost}\} \quad (\mathbf{28})$$

A- = {{ min v_ij |j ∈ J_benefit ; max v_ij| j ∈ J_cost }

Step 5: Calculating Separation Measures

$$\mathbf{S_+^i} = \sqrt{\sum_{\mathbf{j=1}}^{\mathbf{n}} (\mathbf{v_{ij}} - \mathbf{v_j} +)\mathbf{2}} \quad (\mathbf{29})$$

$$\mathbf{S_-^i} \sqrt{\sum_{\boldsymbol{j=1}}^{\boldsymbol{n}} (\mathbf{v\_ij} - \mathbf{v\_j} -)\mathbf{2}}$$

Step 6: Computing the Closeness Coefficient

$$\mathbf{CC_i} = \frac{\mathbf{S_-^i}}{\mathbf{S\_i} + + \mathbf{S\_i} -} \quad (\mathbf{30})$$

A beam configuration with a higher CC_i value is closer to the optimal performance vector.

3.3 Application to Parametric Beam Results

Using results derived from the vibration analysis of composite curved beams, with span L = 1 m and curvature ratios L/R = 0.2 and L/R = 0.4, values for the first four natural frequency modes, static deflections (calculated through beam theory), and masses (M_o = 2.7 kg; ρ = 1580 kg/m³) were determined. Cost estimations were based on approximate material volume and unit pricing models, such as cost per kilogram of CFRP. These values were used to construct the decision matrix, which was then analysed using the TOPSIS algorithm to produce a ranked sequence of beam configurations. For example, a beam with a curvature ratio of L/R = 0.4 may exhibit improved weight characteristics while presenting a slight reduction in stiffness. The proposed framework effectively facilitated the identification and justification of performance trade-offs, based on the proximity of each alternative to the ideal solution vector.

3.4 Engineering Implications and Decision Support

The incorporation of MCDM through the TOPSIS method signifies a transition from traditional single-metric design approaches to multi-objective decision-making frameworks that account for practical constraints and stakeholder priorities. This methodology is especially critical in the following contexts:

• High-speed rail systems, where elevated dynamic amplification may result in structural fatigue and service interruptions.

• Aerospace structures, where controlling both weight and vibration is essential for optimising fuel efficiency and maintaining structural integrity.

This framework offers engineers a quantifiable, transparent, and reproducible tool for evaluating composite beam alternatives, thereby supporting informed decision-making during both the initial design phase and retrofit evaluations.

3.5 Proposed Integrated Framework

To facilitate the identification of the optimal design, the following framework integrates the analysis of the dynamic response with MCDM methods. With this integrated approach, performance-based comparison of design alternatives is made against essential measures like stiffness, weight, deflection, and cost.

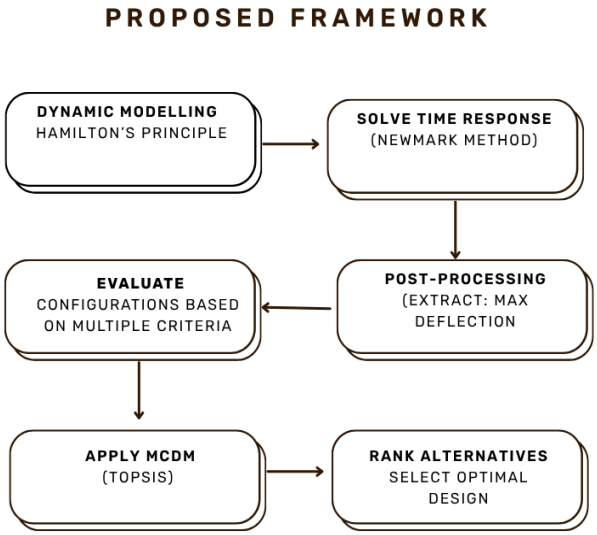

Fig.2: Proposed Decision-Support Workflow used in this Study.

4. Results and Discussion

This part comprises the presentation of the numerical outcomes, attempting to address the

effect of various parameters on the non-uniform system's dynamic response as a result of the moving mass presence. Before the presentation of the research findings, it was confirmed using the available references towards the assurance of the accuracy of the findings. Upon the successful corroboration, the effect of various variables on the non-uniform dynamic behavior of the curved composite beam in the presence of the moving mass was analyzed.

4.1 Validation

To verify the reliability of the current results, a comparative analysis was conducted involving the fundamental frequencies of the free vibration response of the composite curved beam. These were evaluated against those reported in a previous benchmark study [34]. The outcomes of this validation process, illustrated in Figure 3, confirm the precision of the present model through close correspondence with the reference data.

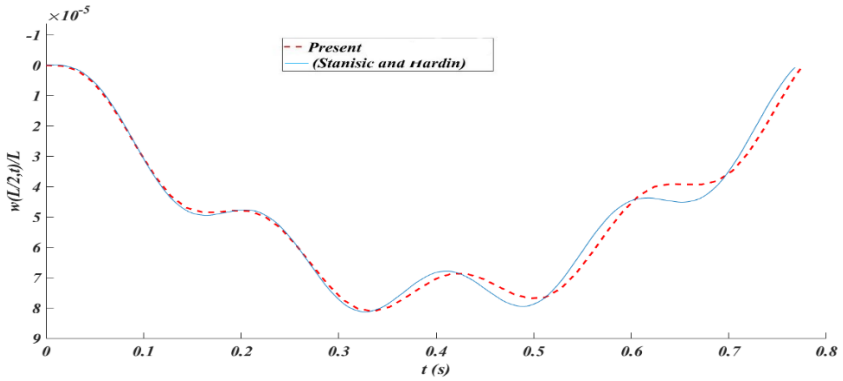

Fig.3: Validating the Dynamic Responding Related to One-Layered Beam to Dynamic Mass [32].

The geometric specifications of the beam, along with the material properties utilized in the analysis are presented in Table 1.

Table 1
Mechanical Properties of the Composite Beam being Curved

$L(m)$	$b(m)$	$h(m)$	$E_{11}(GPa)$	$E_{22}(Gpa)$	$G_{12}(GPa)$	ν	$\rho(\frac{kg}{m^3})$
1	0.05	0.025	200	8.96	7.1	0.3	1580

Table 2 contains a comparative evaluation of the dimensionless natural frequencies, which supports the validation of the model. To further validate the dynamic response of the curved beam under a moving mass, the deflection characteristics of a single-layered beam were systematically compared with previously reported analytical results, particularly those documented in [32].

Table 2
Comparative Analysis of Dimensionless Natural Frequency for a Composite Beam being Curved with a Simple Support for the Porcelain Layer

	$\frac{L}{R}=0.2$		$\frac{L}{R}=0.4$	
n	Present	[16]	Present	[16]
1	3.2887	3.283	3.229	3.224
2	13.02	12.94	12.96	12.89
3	28.65	28.29	28.59	28.23
4	49.43	48.39	49.38	48.34

The material specifications and geometric parameters used in this validation exercise are

summarized in Table 3.

Table 3
The Geometric Mechanical Features of a Single-Layer Beam for Validation

$L(m)$	$\frac{b}{L}$	$\frac{h}{L}$	$E(GPa)$	ν	$\rho(\frac{kg}{m^3})$	$M_0(kg)$	$V(\frac{m}{s})$
20	0.02	0.05	07	0.25	2700	2.7	25

4.2 Parametric Results and Engineering Implications

Upon completing the model validation, multiple parameters were systematically altered to evaluate their influence on the dynamic response of the composite curved beam subjected to a moving mass. The resulting observations offer valuable insights applicable to engineering design and policy formulation.

Effect of Beam Curvature (L/R Ratio): An increase in curvature was observed to decrease the dynamic amplification factor, indicating enhanced load distribution efficiency. Nonetheless, excessive curvature induced localised stress concentrations, necessitating a balance between structural stiffness and manufacturability constraints.

Influence of Moving Mass Velocity: Elevated velocities of the dynamic mass resulted in pronounced mid-span deflections and heightened stress responses. This effect is particularly relevant for applications in railway bridge decks and high-speed transportation infrastructures, where operational speeds can vary significantly.

Material Configuration (Layer Orientation): Variations in fibre orientation within the laminate structure produced notable differences in both damping characteristics and stiffness behaviour. Laminates with balanced layups featuring alternating fibre angles exhibited superior dynamic response, underlining the importance of orientation design in optimising performance.

4.3 MCDM-Based Evaluation of Design Alternatives

To complement the parametric analysis, a MCDM framework was utilised to methodically evaluate and rank different beam design configurations according to their performance under moving mass conditions. The assessment criteria included:

- Dynamic Amplification Factor (DAF) – to minimize structural vibration
- Maximum Mid-Span Deflection – to ensure serviceability
- Natural Frequency Stability – to avoid resonance
- Material Cost Estimate – to reflect practical implementation
- Manufacturing Feasibility Score – derived from curvature ratios and layup complexity.

The TOPSIS method was applied to normalise the selected criteria, assign weights reflecting engineering priorities, and generate a ranking of various beam configurations. These configurations included combinations of:

- Lamination Schemes (e.g., [0/90/0], [0/±45/90], symmetric and antisymmetric)
- Span-to-Radius Ratios (L/R) = 0.2, 0.3, 0.4
- Velocities of Moving Mass = 10 m/s, 20 m/s, 30 m/s.

All of the design options were assigned performance scores, the latter of which appear in Table 4. The highest-scoring setup is the most well-balanced design, striking the optimal combination of the dynamics of performance as well as utilitarian considerations of weight, stiffness, and economy. Overall, ranking-wise, Alternative A1, intermediate in curvature, smaller in velocity, is the best-performing of all, optimal for low-cost, dynamically stable applications, e.g., lightweight pedestrian bridges or low-speed railway crossers. In contrast, configurations exposed to high-speed loading or

pronounced curvature (A3) received the lowest rankings, reflecting an increased susceptibility to vibration-related damage. This integration of MCDM facilitates a quantitative evaluation of trade-offs, thereby strengthening the engineering decision-making process in selecting optimal beam configurations within practical constraints.

Table 4
MCDM Ranking of Design Alternatives using TOPSIS

Al ternative ID	Lamination	L/R	Velocity (m/s)	DAF Score	Deflection	Cost	Manufacturing Score	Final Rank
A1	[0/90/0]	0.2	10	0.18	0.25	Low	High	1
A2	[0/±45/90]	0.3	20	0.35	0.31	Med	Med	3
A3	[0/90/0]	0.4	30	0.42	0.45	High	Low	5
A4	[0/±45/90]	0.2	20	0.25	0.28	Med	High	2
A5	[0/90/0]	0.3	30	0.39	0.41	High	Med	4

5. Numerical Findings

5.1 Convergence Analysis for the Dynamic Responding of the Composite Curved Beam

The convergence behaviour related to the dynamic response analysis of a composite curved beam subjected to a moving mass is shown in Figure 4. This figure demonstrates how the numerical solution stabilises as the number of modes or terms in the series, denoted by N, increases. It is observed that the displacement responses become effectively identical once N reaches a value of 3. This indicates that the solution achieves sufficient accuracy beyond this point with minimal additional computational effort. Based on this convergence analysis, all subsequent simulations and result interpretations in this study use N = 3. This choice balances computational efficiency with numerical precision. The truncation at this mode number confirms the robustness of the adopted method and facilitates dynamic evaluations of the beam across varying moving mass and curvature conditions. Furthermore, the observed convergence supports the parameter selection for the optimisation phase, where computational economy is important. This approach ensures that the proposed decision-support framework remains practical for iterative assessments within a multi-objective context, particularly when combined with metaheuristic optimisation algorithms.

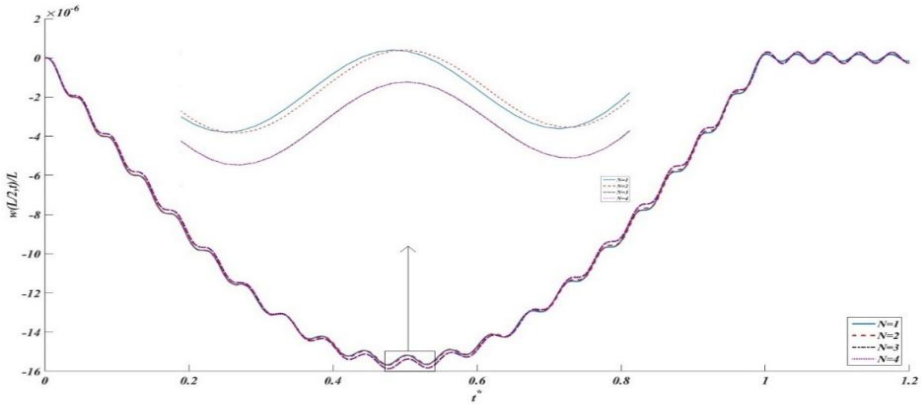

Fig.4: Dynamic Responding Related to the Curved Composite Beam When Depended upon the Non-Constant Mass: Convergence Analysis.

5.2 Examining the Impacts of Differing Parameters on the System's Response

This section investigates the dynamic response of the curved composite beam subjected to a non-constant moving mass, focusing on key parameters such as the mass of the moving object, the beam's radius of curvature, the velocity of the moving mass, the modulus of elasticity, the fibre orientation angle, and the material density.

The non-dimensional time parameter is defined as follows:

$$t^* = t\frac{V}{L} \tag{31}$$

The velocity is presumed to be $V = 5\frac{m}{s}$, and the gravitational acceleration is assumed to be $g = 9.81\ \frac{m}{s^2}$ in the results. The mass that's moving is also supposed to be equivalent to M=1 kg and the mass of this beam is equivalent to:

$$m_b = \rho bhL = 1.975kg \tag{32}$$

Figure 5 depicts the dynamic response of the composite curved beam to the moving mass as the mass of the object increases. The figure demonstrates that the maximum dynamic response of the curved beam rises with increasing moving mass, consistent with previous studies. This behaviour is explained by the increase in inertia associated with the larger mass, which in turn intensifies the applied load. This finding highlights the structural response's sensitivity to the inertial effects of the moving mass, emphasising the necessity of precise modelling of mass variations in predictive analyses. Additionally, it underscores the importance of optimising design parameters for composite beam systems frequently subjected to dynamic loading from moving bodies, such as those found in railway and mechanical transport applications.

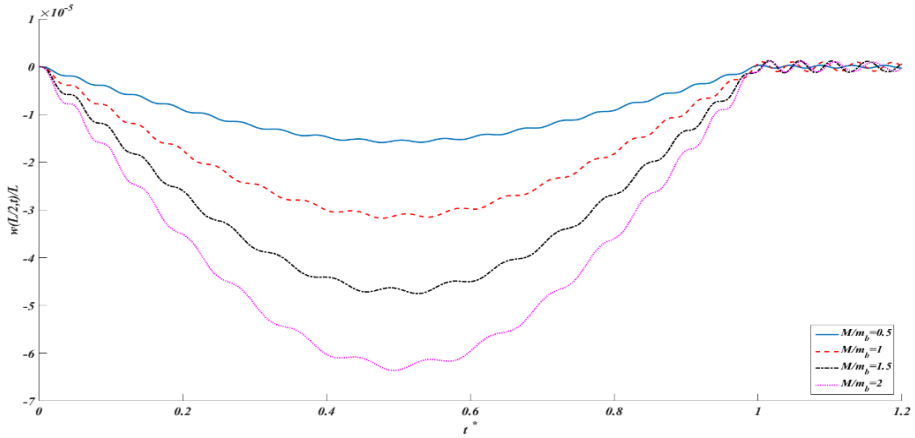

Fig.5: The Impact of Mass Size on the Dynamic Responding of the Composite Curved Beam in the Form of the Layered $[0/90]_2$ under the Non-Constant Mass.

Figure 6 illustrates the influence of velocity on the dynamic response of a non-constant moving mass applied to a composite curved beam. With increased moving object speed, the displacement of the beam initially increases, mirroring increased excitation as the kinetic energy grows. This pattern is evident until the threshold speed for deflection is obtained, at which point the displacement starts to diminish. It was discovered that the maximum deflection increased by about 3.7% with increased object speed, showing a non-linearity in this relationship between structure response and object speed. This indicates a resonance-like effect at medium speeds, after which there is inertial stabilisation at increased velocities. Besides amplitude, the time duration of forced vibration is also notably affected by the changes in speed of the object. With increased object speed, the time duration in which the beam has large scale oscillations decreases, indicating the relatively fast passage of the load along the structure, reducing the duration of the excitations experienced by the system as well as the time it takes for the system to stabilise. Layup of the composite, given as $[0/90]_2$, is responsible for this characteristic in that it supplies the structure with directional stiffness, further shaping the vibrational response of the system. These results hold particular significance in the optimisation of designs in high speed passage applications across

curved composites in the structural components involved.

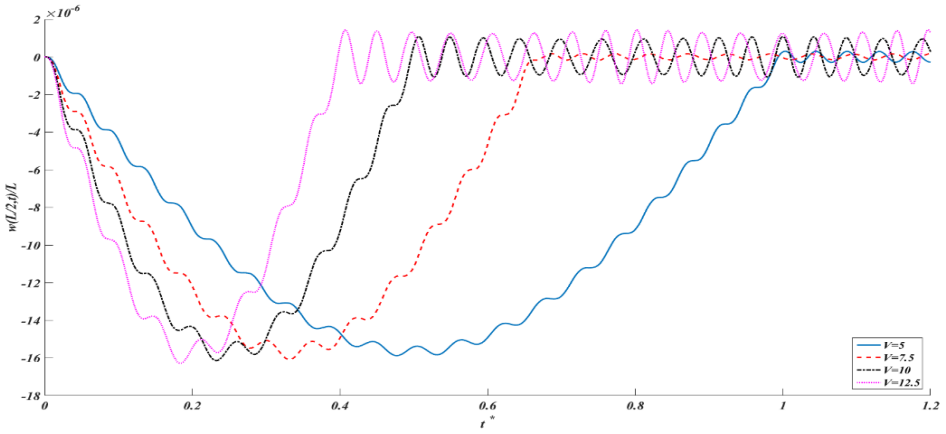

Fig.6: The Influence of Varying Velocity on the Dynamic Responding Related to the Composite Curved Beam in the Form of the Layered $[0/90]_2$ under the Non-Constant Mass.

The influence of varying the modulus of elasticity on the dynamic response of the composite curved beam is examined in Figure 7. The modulus of elasticity plays a pivotal role in defining the structural stiffness of the beam and, consequently, its vibrational response when subjected to a moving mass. When a stiffer material layer, such as porcelain, is introduced, the beam exhibits reduced susceptibility to deformation. This enhancement in stiffness substantially lowers the dynamic displacement experienced by the structure. The results presented in Figure 7 exhibit a clear trend: beams with a higher modulus of elasticity demonstrate significantly reduced deflection across the entire motion path of the moving load. The reduction in displacement becomes more pronounced as the stiffness differential between the composite layers increases. This outcome underscores the critical influence of elastic properties on dynamic performance, particularly in layered composite structures such as the $[0/90]_2$ configuration. The elevated bending stiffness effectively dampens the vibrational response induced by inertial forces from the moving mass, thereby contributing to overall structural stability.

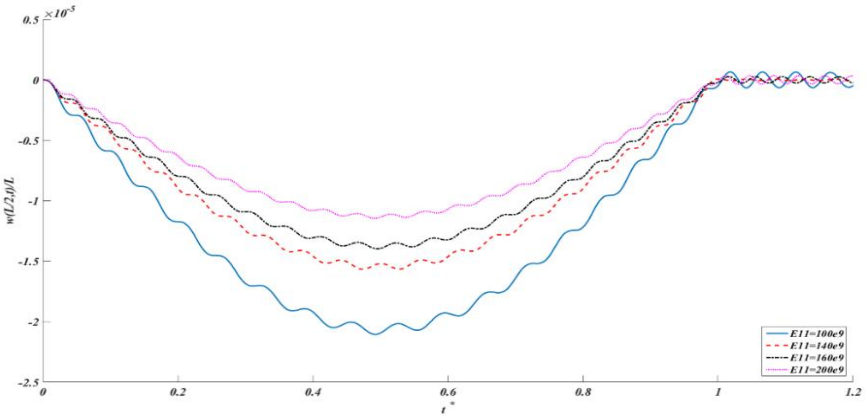

Fig.7: The Influence of Diverse Modulus of Elasticity on the Dynamic Responding of the Composite Curved Beam in the Form of the Layered $[0/90]_2$ under the Dynamic Mass.

From a quantitative perspective, doubling the modulus of elasticity leads to a reduction of approximately 45.55% in maximum displacement. This marked decrease in dynamic deflection confirms the efficacy of enhancing stiffness as a vibration control strategy in composite curved beams. These findings are highly relevant for engineering applications where dynamic performance

is a critical design concern, such as in aerospace, civil infrastructure, and transportation systems, where materials must balance strength, lightness, and vibrational resilience. A practical example includes scenarios involving high-speed rail or heavy vehicular movement across curved bridge decks, where controlling dynamic response through strategic stiffness optimisation is essential. The insights gained here support the development of effective material layering techniques that enhance structural durability, reduce maintenance demands, and improve safety under transient loading conditions.

The dynamic response of the composite curved beam under a non-stationary moving mass is examined with respect to variations in beam length, as illustrated in Figure 8. The results indicate that an increase in beam length leads to a corresponding rise in deflection. This behaviour arises from the inherent reduction in bending stiffness associated with longer spans, rendering them more susceptible to dynamic excitation caused by moving loads. The diminished structural resistance results in greater deformation along the beam's length. Moreover, as the beam's length is increased, the duration of the moving mass's contact with the structure is accordingly increased as well. This increased duration of interaction provides for increased transfer of dynamic as well as inertial force to the beam. With increased exposure, the response of the structure is increased, particularly for the lower-frequency vibration modes of easy excitation in longer beams. This behavior of the beam's length is thus aided by mechanical flexibility as well as increased time intervals of dynamic loading.

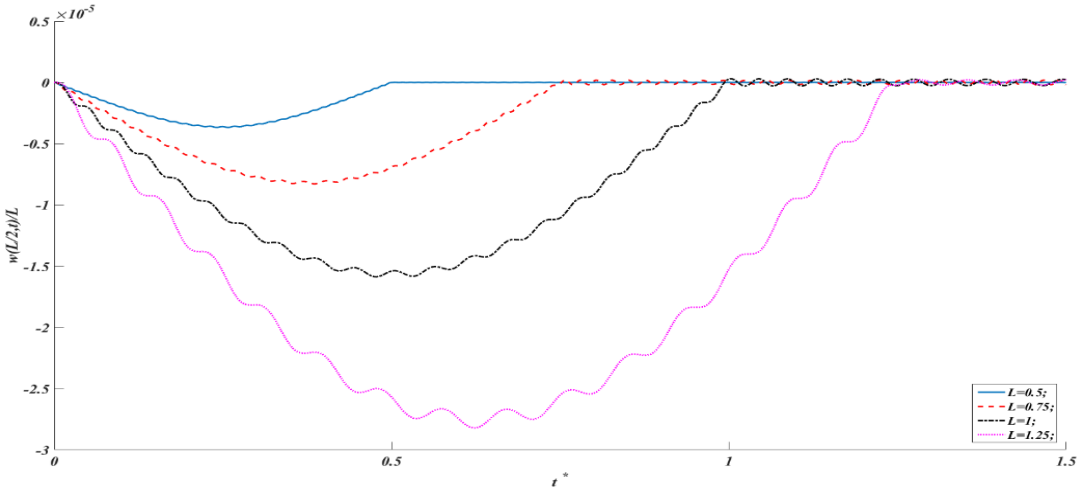

Fig.8: The Influence of Diverse Lengthiness on the Dynamic Responding of the Composite Curved Beam in the Form of the Layered $[0/90]_2$ under the Mass Moving.

The combined effect of reduced stiffness and longer loading duration results in displacement amplitude increasing appreciably for longer beams. Graphical results explicitly reveal that the shortest beam experiences least deformation, while the longest beam exhibits large deflection. This is evidence for the requirement for optimisation of beam length in structural applications for dynamic moving loads. This is true for bridge span design, aerospace structural members, as well as in railway infrastructure design, in which the curvature along with the length conclusively determine the performance in the dynamics regime. Insight of the relationship between beam-length and dynamic deflection can impart wiser structural design optimisation. Optimum beam geometry in the form of optimal length, optimal curvature, as well as optimal material stiffness, must, therefore, be optimised to enable resistance in the face of transient loading conditions. These findings influence prudent engineering choices for the purposes of improving structural integrity as well as improving safe operating conditions in reality applications.

Figure 9 depicts the influence of the variation of the radius of curvature on the structural response of a curved composite beam to a moving mass load. Increasing the radius decreases the curvature, in effect, reducing the geometry more towards that of a straight beam. Results indicate that this geometric variation, although relatively modest, produces a quantifiable impact for the structural dynamic performance. Specifically, the increase in the radius results in increased deflection of the beam, thus corroborating the structural vulnerability to variation in the degree of curvature when the conditions of load are of the dynamic kind. This is attributable to the increased rigidity in the direction of bending that is associated with the larger radii. A smaller extent of curvature thus implies a more flexible geometric outline, which is intrinsically less resistant to excitations of the dynamic kind. Consequently, for the same moving load, the displacement of the latter is larger for the beam of the increased radius. This magnitude of the differential deflection is, on the whole, not large, but the result is systematic, measurable, and thus corroborates the fact that ostensibly minor variations in the extent of the degree of curvature can impact structural response when the system is constrained by non-stationary, dynamic conditions of loading.

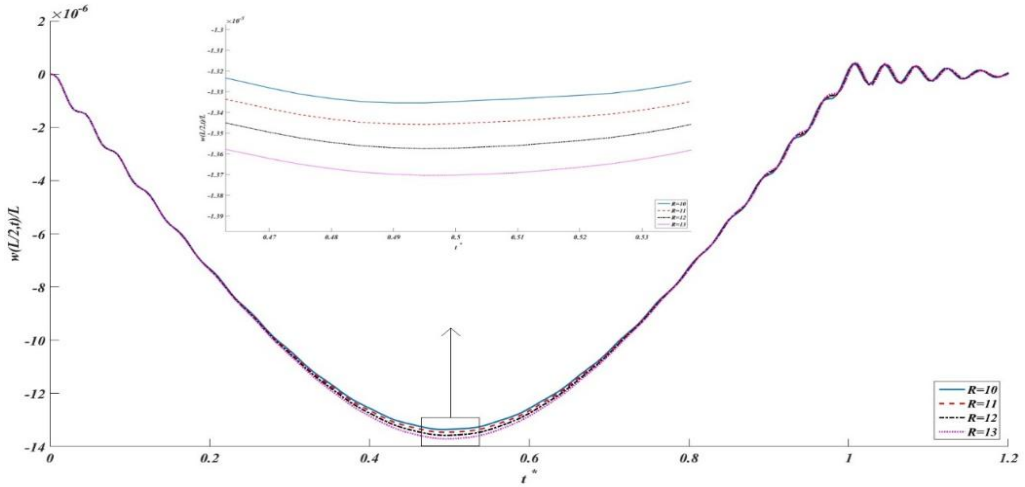

Fig.9: The Influence of Varying Lengthiness on the Dynamic Responding of the Composite Curved Beam in the Form of the Layered $[0/90]_2$ under the Moving Mass.

The quantitative analysis shows that the increase in the radius of curvature by 30% corresponds to about 2.62% deflection rise of the beam. Whilst this is relatively moderate, it further manifests the significance of optimisation of the curvature during the design of the composite structural components. This is of particular significance in applications whereby mechanical effectiveness as well as geometric flexibility is essential. The findings further indicate that the curvature is not only merely a geometric parameter but also provides the determinant of the dynamic performance of the system, particularly in applications whereby moving mass loads come into action. Such findings present profound applications in structural applications involving curved railway bridges, arched transport platforms, as well as aerospace components of support, whereby the direct deflection as well as vibrational response is directly influenced by the curvature. In layered composite structures, fine-tuning the radius of curvature contributes to a more effective balance between stiffness and flexibility, enhancing overall performance under varying operational scenarios.

The dynamic response of the composite curved beam, as depicted in Figure 10, demonstrates the effect of varying porcelain layer configurations. The system's range of forced oscillations for layering $[45/-45/-45/45]$ and $[0/90/90/0]$ has the highest and lowest values, respectively, as indicated by the results. Modifying the fibre layering arrangement directly influences the stiffness

characteristics of the composite beam, thereby affecting its overall flexibility.

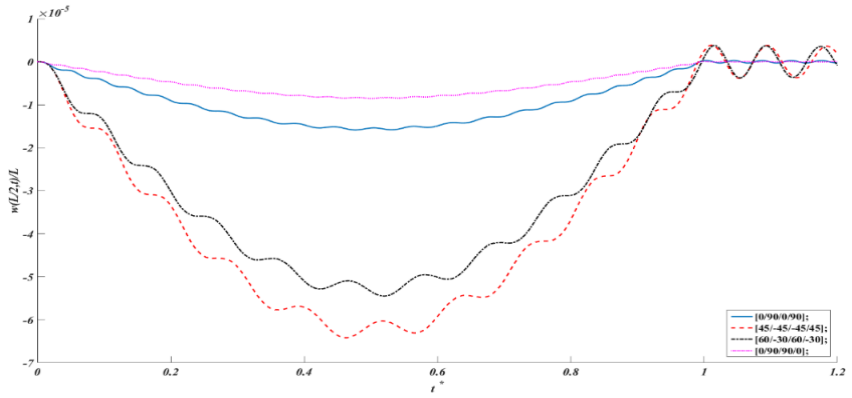

Fig.10: Dynamic Responding of the Composite Beam Being Curved under Moving Mass: Influence of Various Porcelain Layers.

Figure 11 illustrates the influence of material density variation on the dynamic response of a curved composite beam subjected to a moving mass. The analysis considers how changes in density affect the beam's displacement profile and vibration characteristics. The deflection curves corresponding to different densities appear closely aligned, indicating that variations in density have a minimal effect on the beam's maximum dynamic displacement under the given loading conditions. While the deflection amplitude is largely unaffected, the vibrational frequency of the system is considerably affected by changes in density. Increasing the material density makes the natural frequencies of the beam lower accordingly, largely due to the increase in inertial resistance. This effect is evident in the mode shapes of the vibration waveform for different cases of density. This response is in line with classical vibration theory, which states that while the added mass need not necessarily affect displacement adversely in the presence of dynamic excitation, it always has the effect of reducing natural frequencies.

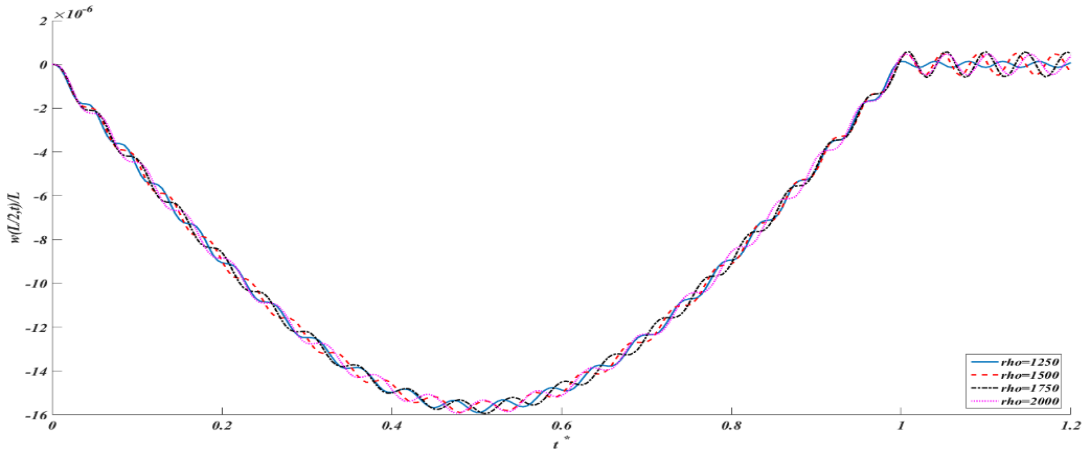

Fig.11: The Influence of Various Density on the Dynamic Responding Related to the Composite Curved Beam in the Form of the Layered $[0/90]_2$ under the Mass Moving.

This finding has design implications for engineers seeking to optimise the dynamics of composite curved beams. Whilst displacement behaviour is significantly regulated by flexural stiffness, material density is the fundamental parameter in the alteration of resonance features. In this context, density is an effective design parameter for adjusting vibrational frequencies without significant deformation control when subjected to dynamic loading. This separation of displacement control based on stiffness from mass-induced frequency variation has particular applicability in

precision engineering applications. Displacement responses remain significantly controlled by the beam's rigidity, whilst frequency tuning of the dynamics is more reliant upon the mass distribution of the structure. This separation provides for the design of selective optimised density strategies in which vibration modes can be changed without compromising the structural performance in response to transient loads. Such design strategies have particular applicability in aerospace, civil engineering, and car.manufacturing applications, in which the suppression of vibration as well as frequency control is of significance. Manipulation of the vibrational characteristics via the adjusting of density provides for the design of intelligent composite systems for vibration-intensive applications. Specifically, the control of the material density as applicable affords resonance mitigation in applications involving periodic or variable dynamic loading. Thus, the inclusion of density-optimised composite ply applications provides for the design of superior vibrational control without the compromise of structural deflection performance or stability.

6. Conclusion

The present study focused on the dynamic analysis of a composite curved beam subjected to a travelling mass. The displacement response was investigated using first-order shear deformation theory. To derive the governing equations of motion, Hamilton's principle was systematically applied. These partial differential equations were addressed in the spatial domain using Navier's analytical technique, while the Newmark method was employed in the temporal domain to capture time-dependent behaviour under simply supported boundary conditions applied at both ends of the beam. The dynamic performance of the beam was examined across a range of influential parameters, including the magnitude of the moving mass, its velocity, beam length, elastic modulus, curvature radius, lamination angle, and material density. The principal findings of this investigation are summarised as follows:

- An increase in the moving mass significantly amplifies the dynamic deflection of the beam. Specifically, when the ratio of moving mass to beam mass is doubled, the maximum deflection increases by approximately 99.87%.
- With rising velocity of the moving mass, the beam exhibits a moderate increase in deflection, accompanied by a notable reduction in the duration of forced vibration, indicating a shorter excitation period.
- By incorporating the $[0/90]_2$ porcelain layer into the beam, the bending rigidity increases, resulting in reducing the locomotive elasticity of the beam. Specifically, the elasticity of the beam decreases by 45.55% when the modulus of elasticity is doubled.
- The dynamic deflection increases by 330.52% when the lengthiness of the composite curved beam is doubled, as beam's deflection also rises up considerably.
- The deflection of the beam, dynamically, increases marginally as radius gets increasing.
- The dynamic responding of the composite curved beam is significantly influenced by the porcelain layers $[45/-45/-45/45]$ and $[0/90/90/0]$, which produce the maximum and lowest dynamic spring values, respectively.

The engineering significance of the parametric findings offers practical design insights. An increase in the curvature ratio (L/R) enhances the distribution of applied loads across the beam span, although this benefit is offset by the emergence of localised stress concentrations. This necessitates a careful balance between curvature and stiffness in the structural configuration. Increased moving mass velocities yield increased mid-span deflection as well as increased internal stresses, of immediate design relevance in high-speed transport deck as well as rail bridge applications. The laminate's layer orientation is revealed as the dominant design variable, with

balanced configurations demonstrating enhanced stiffness as well as damping behavior. Also, the ensuing convergence characteristics constitute evidence of the parameter choices adopted during the optimisation process, of specific benefit in schemes based upon the deployment of metaheuristic optimisation algorithms. The results confirm the system's strong inertial effect sensitivity due to the moving mass, consequently further underscoring the requirement for accurate modelling for the purposes of dynamic simulation as well as the selective beam property tailoring for operational loading scenarios.

These results present specific interest for engineering applications in the real world, particularly in aerospace and transport infrastructure applications, in which the composite curved beam often experiences transient dynamics loading. Changes in beam curvature and beam length present substantial structural resilience improvements along with operational performance enhancement provisions. Differentiation of stiffness-controlled displacement response against mass property-controlled frequency behaviour provides for the intentional design potential in material density so that it is materially varied in select applications to control the vibration modes without detrimental impact upon structural deformation upon load conditions. This potential enables the realization of intelligent composites in select vibration sensitive applications including arched bridge decks, curved rail supporting members, as well as aerospace structural components. In order to aid rational design selection, the MCDM approach was adopted, using the TOPSIS amongst others. This facilitated the systematic design ranking of design options against performance parameters involving the dynamic deflection, stiffness, mass per unit length, as well as the costing parameters. MCDM application provided for the in-depth evaluation of design trade-offs, thus facilitating optimal decisions with regards to beam span, radius of curvature, fibre orientation, as well as the material density. This unifying strategy closes the theoretical results of the vibration analysis with the engineering design, making the findings of the study applicable to the transport as well as the structural system advancements.

7. Implications

Results of this research hold broad implications for structural engineering, specifically in the design and analysis of composite curved members under the action of dynamic loading. Through the identification of the effect of design parameters of central importance—the magnitude of moving mass, velocity, beam length, radius of curvature, elastic modulus, and laminate configuration—the research provides engineers with essential information to optimise structural performance in high-demand sectors like transport infrastructure, aerospace systems, and robot applications. Analysis shows that careful stacking sequence selection of the laminate, together with selective utilisation of the elastic moduli, can substantially suppress unwanted oscillatory responses, hence improving structural stability as well as operational efficiency. These findings hold particular significance in the face of increasing subjecting of engineering structures to high-speed as well as transient dynamic loads. The research provides the foundation for the design of the composites system that is not merely efficient in responding to these kinds of loads but also sustainable for longer service lifetimes. Besides the design practices, the findings further offer useful information for the management of infrastructures. For one, for example, the parameter sensitivities of increased deflection resulting from high values can inform the planning of effective maintenance, allowing for the design of proactive inspection programmes aimed at reducing the risk of failure. From the investment vantage, the findings also inform the design of the composites system whose utilisation is justified based on the attainable performance improvements in the response dynamics, hence pertinent to high-speed rail, aerospace applications, among others, in which load-induced vibrational effects present key design issues. Through this research, the linkages between the

advanced modeller's tools as well as performance-based design practices narrow, yielding the potential for the design of composites system that is efficient, sustainable, as well as optimised in terms of lifecycle performance.

8. Future Directions

Future studies could expand upon the findings presented herein by exploring the following research directions:

- Inclusion of Damping Effects: Subsequent research must incorporate the idea of adding damping mechanisms in the calculation of the curved composite beam's dynamic response. Since structural systems of real applications dissipate energy, the incorporation of damping characteristics would critically enhance the accuracy as well as realism of numerical simulations, leading to design recommendations as well as prediction capabilities that are more precise.
- Multiple Moving Masses and Variable Velocities: Future research must generate scenarios of multiple moving masses traveling at variable velocities. This would more closely resemble actual service conditions, e.g., as is the case in bridge applications during double or simultaneous passage of vehicles or in machine-based industries involving multiple dynamic components in motion at the same time.
- Development of New Materials: More research can further explore the performance of high-performance, new-generation composite materials, such as FGMs, and Nano-reinforced polymers. These new-age materials hold bright prospects for the improvement of mechanical behavior, enhancing structural responses against new-age loads, thus adding innovation in material science as well as design strategies in the fields of engineering.
- Nonlinear Behaviour and Large Deformations: With the foundation of the current research, further contributions can delve into the nonlinear dynamic behaviour of curved composite members, specifically large displacement phenomena, geometric nonlinear effects, as well as instability effects. These factors hold high priority for the overall system behaviour consideration in the presence of high-intensity dynamic excitations.
- Practical Field Tests and Experimental Work: Empirical validations in the large-scale laboratory tests along with in-situ field trials need to be conducted in order to validate the computation outcomes derived here. Practical investigations would bridge the gap between theoretical modelling as well as implementation, further enhancing the proposed applicability and validity of the adopted numerical formulations.

References

[1] Al-Rubaye, S., Tsourdos, A., & Namuduri, K. (2023). Advanced air mobility operation and infrastructure for sustainable connected evtol vehicle. *Drones*, *7*(5), 319. https://doi.org/10.3390/drones7050319

[2] Aldarraji, I., Kakei, A. A., Ismaeel, A. G., Tsaramirsis, G., & Patel, A. (2022). Dynamics modeling and motion simulation of a segway robotic transportation system. In *Intelligent Computing Techniques for Smart Energy Systems: Proceedings of ICTSES 2021* (pp. 83-91). Springer. https://doi.org/10.1007/978-981-19-0252-9_9

[3] Alkhawaldeh, S. M. A. (2024). Hybrid RNN and metaheuristic approach for modeling and optimization of seismic behavior in thin-walled rectangular hollow bridge piers. *Asian Journal of Civil Engineering*, *25*(3), 2399-2413. https://doi.org/10.1007/s42107-023-00915-8

[4] Asgarieh, E., Moaveni, B., & Stavridis, A. (2014). Nonlinear finite element model updating of an infilled frame based on identified time-varying modal parameters during an earthquake. *Journal of Sound and Vibration*, *333*(23), 6057-6073.

https://doi.org/10.1016/j.jsv.2014.04.064

[5] Aznaw, G. M. (2025). Advances in Composite Structures: A Systematic Review of Design, Performance, and Sustainability Trends. *Composite Materials*, *9*(1), 1-17. https://doi.org/10.11648/j.cm.20250901.11

[6] Biglari, H., Teymouri, H., & Shokouhi, A. (2024). Dynamic Response of Sandwich Beam with Flexible Porous Core Under Moving Mass. *Mechanics of Composite Materials*, *60*(1), 163-182. https://doi.org/10.1007/s11029-024-10181-7

[7] Chen, D., Yang, J., & Kitipornchai, S. (2016). Free and forced vibrations of shear deformable functionally graded porous beams. *International journal of mechanical sciences*, *108*, 14-22. https://doi.org/10.1016/j.ijmecsci.2016.01.025

[8] Chen, X., Yang, L., Gong, Y., & Liu, K. (2025). Lightweight design of multi-material body structure based on material selection method and implicit parametric modeling. *Proceedings of the Institution of Mechanical Engineers, Part D: Journal of Automobile Engineering*, *239*(8), 3382-3404. https://doi.org/10.1177/09544070241249206

[9] Esen, I. (2019). Dynamic response of a functionally graded Timoshenko beam on two-parameter elastic foundations due to a variable velocity moving mass. *International journal of mechanical sciences*, *153*, 21-35. https://doi.org/10.1016/j.ijmecsci.2019.01.033

[10] Freidani, M., & Hosseini, M. (2020). Elasto-dynamic response analysis of a curved composite sandwich beam subjected to the loading of a moving mass. *Mechanics of advanced composite structures*, *7*(2), 347-354. https://doi.org/10.22075/macs.2020.19275.1231

[11] Gara, F., Nicoletti, V., Carbonari, S., Ragni, L., & Dall'Asta, A. (2020). Dynamic monitoring of bridges during static load tests: influence of the dynamics of trucks on the modal parameters of the bridge. *Journal of Civil Structural Health Monitoring*, *10*(2), 197-217. https://doi.org/10.1007/s13349-019-00376-1

[12] Hassani, S., Mousavi, M., & Gandomi, A. H. (2021). Structural health monitoring in composite structures: A comprehensive review. *Sensors*, *22*(1), 153. https://doi.org/10.3390/s22010153

[13] Jiang, S., & Tahmasebinia, F. (2025). Developing New Design Procedure for Bridge Construction Equipment Based on Advanced Structural Analysis. *Applied Sciences (2076-3417)*, *15*(5). https://doi.org/10.3390/app15052860

[14] Kadivar, M., & Mohebpour, S. (1998). Finite element dynamic analysis of unsymmetric composite laminated beams with shear effect and rotary inertia under the action of moving loads. *Finite elements in Analysis and Design*, *29*(3-4), 259-273. https://doi.org/10.1016/S0168-874X(98)00024-9

[15] Karimi-Asrami, A., & Jafari-Talookolaei, R.-A. (2025). Free and forced vibration analysis of functionally graded porous frames. *Engineering Computations*, *42*(4), 1417-1446. https://doi.org/10.1108/EC-10-2024-0981

[16] Kumar, S., & Nallasivam, K. (2025). Dynamic response of a PSC box-girder bridge impacted by high-speed train load using the finite element approach. *Innovative Infrastructure Solutions*, *10*(1), 22. https://doi.org/10.1007/s41062-024-01845-3

[17] Li, S., & Ren, J. (2018). Analytical study on dynamic responses of a curved beam subjected to three-directional moving loads. *Applied Mathematical Modelling*, *58*, 365-387. https://doi.org/10.1016/j.apm.2018.02.006

[18] Li, X., Zhai, H., & Zhao, D. (2023). Out-of-plane dynamic response of elliptic curved steel beams based on the precise integration method. *Buildings*, *13*(2), 368. https://doi.org/10.3390/buildings13020368

[19] Lin, S.-M., & Lee, K.-W. (2016). Instability and vibration of a vehicle moving on curved beams with different boundary conditions. *Mechanics of Advanced Materials and Structures*, *23*(4),

375-384. https://doi.org/10.1080/15376494.2014.981618

[20] Liu, Z., Zhang, Z., & Ritchie, R. O. (2020). Structural orientation and anisotropy in biological materials: functional designs and mechanics. *Advanced Functional Materials*, *30*(10), 1908121. https://doi.org/10.1002/adfm.201908121

[21] Monfared, V., Ramakrishna, S., Alizadeh, A. a., & Hekmatifar, M. (2023). A systematic study on composite materials in civil engineering. *Ain Shams Engineering Journal*, *14*(12), 102251. https://doi.org/10.1016/j.asej.2023.102251

[22] Mosleh, A., Costa, P. A., & Calçada, R. (2020). A new strategy to estimate static loads for the dynamic weighing in motion of railway vehicles. *Proceedings of the Institution of Mechanical Engineers, Part F: Journal of Rail and Rapid Transit*, *234*(2), 183-200. https://doi.org/10.1177/0954409719838115

[23] Mu, N., Xin, P., Wang, Y., Cheng, C., Pedrycz, W., & Chen, Z.-S. (2023). Vulnerability analysis of China's air and high-speed rail composite express network under different node attack strategies. *Annals of operations research*, 1-35. https://doi.org/10.1007/s10479-023-05655-1

[24] Parvaneh, F., & Hammad, A. (2024). Application of Multi-Criteria Decision-Making (MCDM) to select the most sustainable Power-Generating technology. *Sustainability*, *16*(8), 3287. https://doi.org/10.3390/su16083287

[25] Ramteke, P. M., & Panda, S. K. (2021). Free vibrational behaviour of multi-directional porous functionally graded structures. *Arabian Journal for Science and Engineering*, *46*(8), 7741-7756. https://doi.org/10.1007/s13369-021-05461-6

[26] Sahoo, P. R., Samal, S., & Kar, S. (2025). Transient analysis of curved plates under moving forces. *Asian Journal of Civil Engineering*, 1-16. https://doi.org/10.1007/s42107-025-01413-9

[27] Sanjrani, A. N., Huang, H. Z., Shah, S. A., Hussain, F., Punhal, M., Narejo, A., & Zhang, B. (2025). High-speed train wheel set bearing analysis: Practical approach to maintenance between end of life and useful life extension assessment. *Results in Engineering*, *25*, 103696. https://doi.org/10.1016/j.rineng.2024.103696

[28] Shao, D., Hu, S., Wang, Q., & Pang, F. (2016). A unified analysis for the transient response of composite laminated curved beam with arbitrary lamination schemes and general boundary restraints. *Composite Structures*, *154*, 507-526. https://doi.org/10.1016/j.compstruct.2016.07.070

[29] Şimşek, M., & Kocatürk, T. (2009). Free and forced vibration of a functionally graded beam subjected to a concentrated moving harmonic load. *Composite Structures*, *90*(4), 465-473. https://doi.org/10.1016/j.compstruct.2009.04.024

[30] Sinha, G. P., & Kumar, B. (2021). Review on vibration analysis of functionally graded material structural components with cracks. *Journal of Vibration Engineering & Technologies*, *9*(1), 23-49. https://doi.org/10.1007/s42417-020-00208-3

[31] Solahuddin, B., & Yahaya, F. (2023). A state-of-the-art review on experimental investigation and finite element analysis on structural behaviour of fibre reinforced polymer reinforced concrete beams. *Heliyon*, *9*(3). https://doi.org/10.1016/j.heliyon.2023.e14225

[32] Stanišić, M. M., & Hardin, J. C. (1969). On the response of beams to an arbitrary number of concentrated moving masses. *Journal of the franklin institute*, *287*(2), 115-123. https://doi.org/10.1016/0016-0032(69)90120-3

[33] Sun, Z. (2025). Moving-load impact of classic hinged-hinged slab beam and demarcation to gravity stretching retention effect. *Frontiers of Structural and Civil Engineering*, *19*(4), 556-566. https://doi.org/10.1007/s11709-025-1172-9

[34] Torelli, G., Fernández, M. G., & Lees, J. M. (2020). Functionally graded concrete: Design objectives, production techniques and analysis methods for layered and continuously graded

elements. *Construction and Building Materials*, *242*, 118040. https://doi.org/10.1016/j.conbuildmat.2020.118040

[35] Wang, D., Sun, C., Liu, X., Wang, Z., & Li, R. (2024). Flow-induced vibration analysis by simulating a high-speed train pantograph. *Applied Sciences*, *14*(11), 4493. https://doi.org/10.3390/app14114493

[36] Wu, H., Dai, Y., & Li, K. (2023). Self-vibration of liquid crystal elastomer strings under steady illumination. *Polymers*, *15*(16), 3483. https://doi.org/10.3390/polym15163483

[37] Wu, Y., Zhou, J., Li, T., Chen, L., Xiong, Y., & Chen, Y. (2024). A review of polymeric heart valves leaflet geometric configuration and structural optimization. *Computer Methods in Biomechanics and Biomedical Engineering*, 1-11. https://doi.org/10.1080/10255842.2024.2410232

[38] Yang, F., Sedaghati, R., & Esmailzadeh, E. (2022). Vibration suppression of structures using tuned mass damper technology: A state-of-the-art review. *Journal of Vibration and Control*, *28*(7-8), 812-836. https://doi.org/10.1177/1077546320984305